Sustainable Cities and Society 93 (2023) 104499

Contents lists available at ScienceDirect

Sustainable Cities and Society

journal homepage: www.elsevier.com/locate/scs

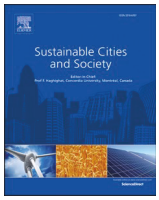

High-resolution thermal exposure and shade maps for cool corridor planning

Isaac Buo [a,*], Valentina Sagris [a], Jaak Jaagus [a], Ariane Middel [b]

[a] Department of Geography, University of Tartu, Estonia
[b] School of Arts, Media and Engineering, School of Computing and Augmented Intelligence, Arizona State University, Tempe, AZ, US

ARTICLE INFO

Keywords:
Mean radiant temperature
urban shade distribution
SOLWEIG
pedestrian thermal comfort
heat action planning

ABSTRACT

Shade is crucial for thermally comfortable cities that promote physical activity. City-wide shade and thermal exposure data are essential for managing heat health risks but are difficult to obtain at fine scales due to limited sensing and modeling capabilities. To address this gap and assist municipalities with "cool corridor" planning, we generated 1-m resolution shade and mean radiant temperature (T_{MRT}) maps from LiDAR point clouds for the Phoenix-Tempe metropolitan area using the SOLWEIG model. T_{MRT} estimates were validated using 763 observations with a mobile human-biometeorological 6-directional setup. SOLWEIG had an overall RMSE of 5.6°C with an error of 6.2°C at open sites, 5.4°C under trees, and 4.4°C in building canyons. Hourly T_{MRT} and shade maps were generated from 7:00 h to 20:00 h for June 27, 2012, a typical clear, dry, calm summer day. We assessed sidewalk shade coverage based on the Maricopa Association of Government's Active Transportation Plan. Only 8% of all sidewalks met the recommended minimum of 20% shade coverage at all times. Less than 50% of all sidewalks met the goal for parts of the day, indicating that the urban area is not walkable during extreme heat. Results from this study will inform municipal cool corridor planning to optimize site selection for heat mitigation.

1. Introduction

Cities worldwide are getting hotter due to anthropogenic changes that impact climate locally and globally. Urban development contributes to the Urban Heat Island effect (Oke, 1981), and extreme heat events are projected to increase in frequency, duration, and intensity due to climate change (Seneviratne et al., 2012). Urban overheating is a significant challenge of the Anthropocene that increases the heat-health burden of urban populations and will lead to an increase in heat-related illness and death if no effective mitigation or adaptation strategies are implemented (Nazarian et al., 2022).

An indispensable strategy to decrease the human heat burden outdoors is to provide shade. Shade is a valuable commodity that reduces UV exposure, thermal discomfort, and heat stress (Aleksandrowicz et al., 2020; Middel et al., 2021; Tabatabaie et al., 2019). Tree shade also enhances the aesthetic quality of streetscapes and influences people's physical activities (Handy et al., 2002). Many municipalities around the globe have centered their heat mitigation plans around street trees to improve thermal comfort for pedestrians and cyclists (Jamei & Rajagopalan, 2017; Speak et al., 2021; Wallenberg et al., 2022). For example, the government of Victoria, Australia, set a goal to increase tree coverage in the City North (Melbourne) from 14% to 40% by the year 2050 (Jamei & Rajagopalan, 2017). Similarly, Brisbane and Bendigo, Australia, implemented the concept of *shadeways,* which includes street trees as an integral part of making commuting comfortable for pedestrians (Butt et al., 2019; Deilami et al., 2020). The City of Phoenix in the hot, dry Southwestern US aims to invest in street trees to reach a 25% tree canopy coverage by 2030. In addition, the City has started a "Cool Corridor" program as part of its Climate Action Plan Framework that aims to establish a network of 100 cool corridors across its districts. Phoenix also became the first city to pledge "Tree Equity," especially increasing tree canopy in economically disadvantaged communities.

To implement shade-centered heat mitigation programs, detailed information on the existing built environment and shade infrastructure is required to estimate human thermal exposure and equitably place new shade infrastructure. In hot, dry environments, the Mean Radiant Temperature (T_{MRT}) has been reliably used as a thermal exposure measure because it quantifies the heat load on the human body and is a significant parameter in assessing outdoor thermal comfort (Hardy & Stoll, 1954). T_{MRT} represents the sum of all short and longwave radiative

* Corresponding author: Isaac Buo, University of Tartu, Vanemuise 46, 51003, Tartu, Estonia
E-mail address: isaac.buo@ut.ee (I. Buo).

https://doi.org/10.1016/j.scs.2023.104499
Received 1 December 2022; Received in revised form 27 February 2023; Accepted 27 February 2023
Available online 12 March 2023

fluxes absorbed by the human body (Höppe, 1992; Lindberg et al., 2008). It is a fundamental input parameter for many biometeorological indices, such as the Physiologically Equivalent Temperature (PET) and the Universal Thermal Climate Index (UTCI) (Crank et al., 2020; Krüger et al., 2014). T_{MRT} is measurable directly by using a set of three net radiometers with sensors facing upward, downward, and the four cardinal directions; or with globe thermometers (Aviv et al., 2022; Guo et al., 2020; Middel et al., 2016; Middel & Krayenhoff, 2019; Vanos et al., 2021).

While T_{MRT} observations provide valuable insight into a person's heat load at a specific time and location, there is a need for spatially explicit, continuous, city-wide T_{MRT} and shade maps to optimize site selection for municipal heat mitigation efforts. The SOlar LongWave Environmental Irradiance Geometry (SOLWEIG) model proposed by Lindberg et al. (2008) simulates high-resolution, spatially explicit shade distributions, radiative fluxes, and T_{MRT} for large areas following the concepts presented in Höppe (1992). SOLWEIG is suitable for estimating T_{MRT} in complex urban settings and has been employed in many geographic contexts (Acero & Arrizabalaga, 2018; Aleksandrowicz et al., 2020; Crank et al., 2020; Gál & Kántor, 2020; Kong et al., 2022). Previous studies have shown that SOLWEIG outperforms other radiation flux models (Chen et al., 2014; Gál & Kántor, 2020; Szucs et al., 2014), but model validation was usually restricted to observational data collected on a single day or several days with only a few sites (Aminipouri et al., 2019; Chen et al., 2014; Gál & Kántor, 2020). Furthermore, no validation study has critically examined the model's accuracy with regard to exposure type and urban forms.

This research aims to produce high-resolution thermal comfort and shade maps for municipal cool corridor planning. First, we evaluate the SOLWEIG model for different exposure types (sun-exposed, shaded by trees, shaded by buildings) and urban forms under hot, dry conditions using extensive field measurements collected over three years in various urban settings. Second, we produce high-resolution hourly T_{MRT} maps for a hot, dry, calm summer day to inform the City of Phoenix Cool Corridor program. Third, we quantify the shade coverage on sidewalks in the Cities of Phoenix and Tempe (the urban core of the Phoenix metropolitan area) on a hot summer day to identify neighborhoods that do not meet the minimum shade coverage recommendation of 20% as outlined in the Maricopa Association of Government's Active Transportation Plan. The study's novelty is three-fold: 1) We perform an unprecedented, extensive validation of the SOLWEIG model using the "gold standard" 6-directional setup for 763 observations collected over three summers at 60 unique sites; 2) We produce hourly T_{MRT} maps for one of the largest areas (1.9 billion 1-m grid cells) the SOLWEIG model has been applied to, and 3) We are the first to separate tree shade from building shade in an analysis of sidewalk shade coverage to identify neighborhoods that do not meet a minimum shade coverage threshold.

2. Study Site

The Phoenix metropolitan area (33°25′00.8" N 111°58′41.5" W) is an amalgamation of 24 cities in Maricopa County, Arizona, USA (Fig. 1). This study focuses on the City of Phoenix and Tempe, two cities in the urban core with an area of 1051 km^2 and 442 census tracts (population of 4,837,000), which account for about 29 % of all census tracts in Arizona. The metropolitan area is in the Sonoran Desert and has a subtropical desert climate (Köppen Climate Classification subtype *Bwh*). Summers in the area are hot, with maximum air temperature reaching or exceeding 38°C between June and August. T_{MRT} can be as high as 76.2 °C at sun-exposed sites (Middel et al., 2021). Phoenix is predominantly an open low-rise Local Climate Zone (LCZ) with an open high-rise downtown area. Tempe is mostly open low-rise with an open mid to high-rise LCZ (Wang et al., 2018).

3. Materials and Methods

This study adopted a two-part approach. First, we modeled T_{MRT} and shade distribution with SOLWEIG (version 2021a) and validated results using in-situ observations for hot summer days. The second part focused on assessing the summertime diurnal shade distribution on sidewalks in the study area based on shade goals set by the Maricopa Association of Government's Active Transportation Plan to improve pedestrian thermal comfort (Fig. 2).

3.1. Mean Radiant Temperature Modeling

To estimate $T_{MRT,}$ SOLWEIG requires a surface model of buildings, a Digital Elevation Model (DEM), and a vegetation canopy height model. In addition, meteorological forcing parameters (air temperature, wind speed, relative humidity, and global solar radiation) are required. SOLWEIG allows users to include direct and diffuse shortwave radiation forcing if available; otherwise, shortwave radiation can be estimated on the-fly using global solar radiation. For this research, both direct and diffuse shortwave radiation components were estimated using SOLWEIG.

The surface models were created using a high-resolution pre-classified LiDAR Point Cloud (LPC) from the United States Geological Survey (USGS). The USGS collected the LPC in 1 km x 1 km overlapping tiles. All points classified as noise were eliminated for each tile, and a 1-m resolution surface model, which we term the Full DSM (FDSM), was created using triangulated irregular networks (Franklin et al., 2006). The FDSM represents the height of the ground and above-ground features. In addition, a DEM for each tile was created using ground points only. A Building Surface Model (BSM) for each tile was generated by extracting pixels in the FDSM masked by buildings using building footprint data from the ASU library for the study site. After the extraction, the BSM was completed by filling the no-data areas (areas outside the building

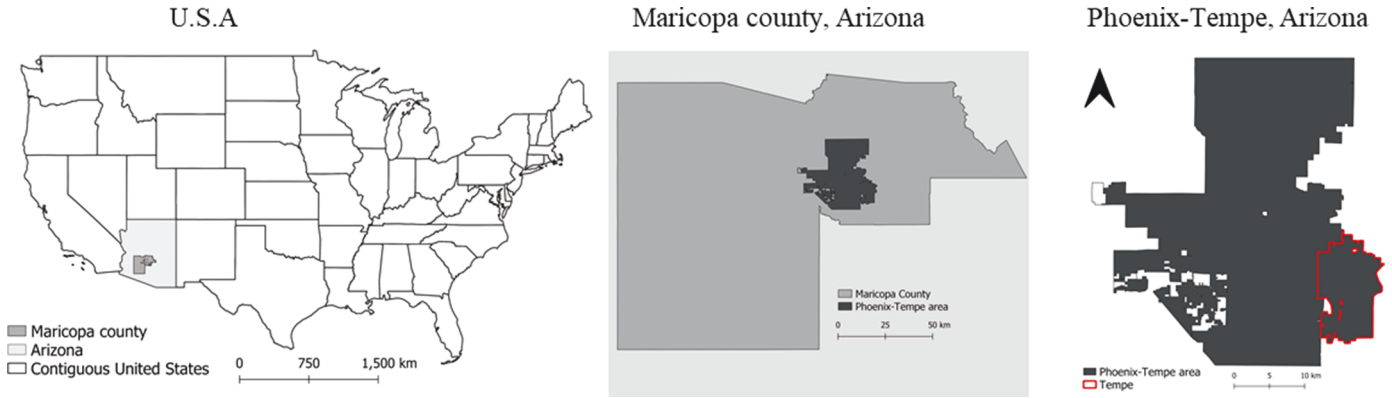

Fig. 1. Map of the study area in the Southwestern US: The City of Phoenix and Tempe in the Phoenix metropolitan area. Maricopa County, Arizona.

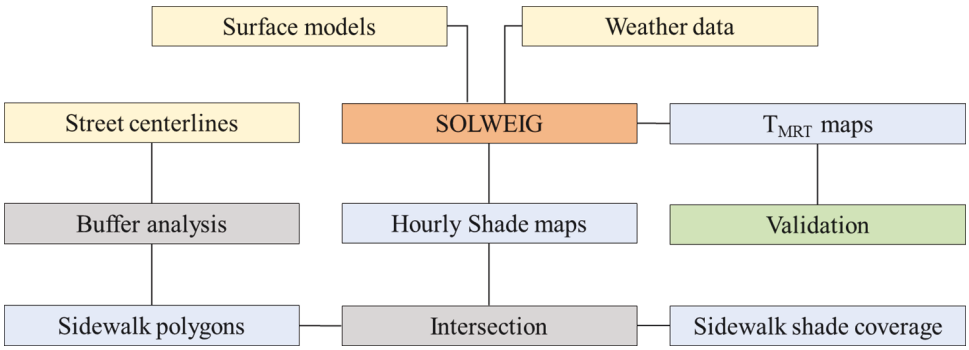

Fig. 2. Workflow of the study, including input data (yellow), GIS operations (grey), validation with MaRTy observations (green), and output data (blue).

footprint) with corresponding data from the DEM. Finally, the Canopy Digital Surface Models (CDSM) for all tiles were created by subtracting the DEM from the FDSM for pixels that were not masked by the building footprints; pixels that were covered by building footprints were set to zero. Furthermore, all pixels with heights less or equal to 1.3 m were set to 0 in the CDSM because we do not consider them high enough to provide shade for the average person standing outdoors.

To estimate T_{MRT} at a location, SOLWEIG determines the mean radiant flux (R_{str}) using Eq. (1), which is a function of short and longwave radiation in six directions, angular factors, and a representation of human posture as suggested by Höppe (1992). The model utilizes surface models (BSM, CDSM, and DEM) to calculate view factors that control the radiation exchange.

$$R_{str} = \zeta_k \sum_{i=1}^{6} K_i F_i + \varepsilon_p \sum_{i=1}^{6} L_i F_i \quad (1)$$

K_i and L_i are the directional short and longwave radiation fluxes, respectively, and F_i are the angular factors between a person and the surrounding surfaces. ζ_k is the absorption coefficient for shortwave radiation, ε_p is the emissivity of the human body. The necessary equations to calculate directional radiation fluxes are given in Lindberg et al. (2008) and Lindberg and Grimmond (2011). The posture of a standing person was adopted for this research, i.e. F_i was set as 0.22 for the cardinal directions and 0.06 for the upward and downward directions. ζ_k and ε_p were set as 0.70 and 0.97, respectively (Lindberg et al., 2008; VDI, 1998). T_{MRT} is estimated in degrees Celsius from R_{str} using the Stefan-Boltzmann law (2):

$$T_{MRT} = \sqrt[4]{\left(R_{str} / \left(\varepsilon_p \sigma\right)\right)} + 273.15 \quad (2)$$

σ is the Stefan-Boltzmann constant (5.67×10^{-8} $Wm^{-2}K^{-4}$).

3.2. Model validation

We used field measurements observed with MaRTy – a mobile human-biometeorological station that measures radiative fluxes in six directions (Middel & Krayenhoff, 2019) to validate T_{MRT} estimates. The observations were made between 07:00 h and 21:00 h Local Standard Time (LST) over 9 hot summer days in 2016, 2018, and 2019 (Middel et al., 2021). In total, 763 observations were collected at 60 unique sites distributed across the Arizona State University (ASU) Tempe campus and in Kiwanis Park, Tempe (Fig. 3). Biometeorological data were acquired under trees, in building canyons, and at open sites. The campus covers 2.6 km^2 and can be classified as an open midrise Local Climate Zone- LCZ (Middel et al., 2016). Kiwanis public park, classified as a scattered trees LCZ (Fig. 3**c**), covers an area of 0.5 km^2 with a lake, sports fields, picnic spots, and playgrounds.

T_{MRT} for the campus and park was calculated using SOLWEIG for the acquisition days and times of the validation data. The model was forced with meteorological data from the Arizona Meteorological Network

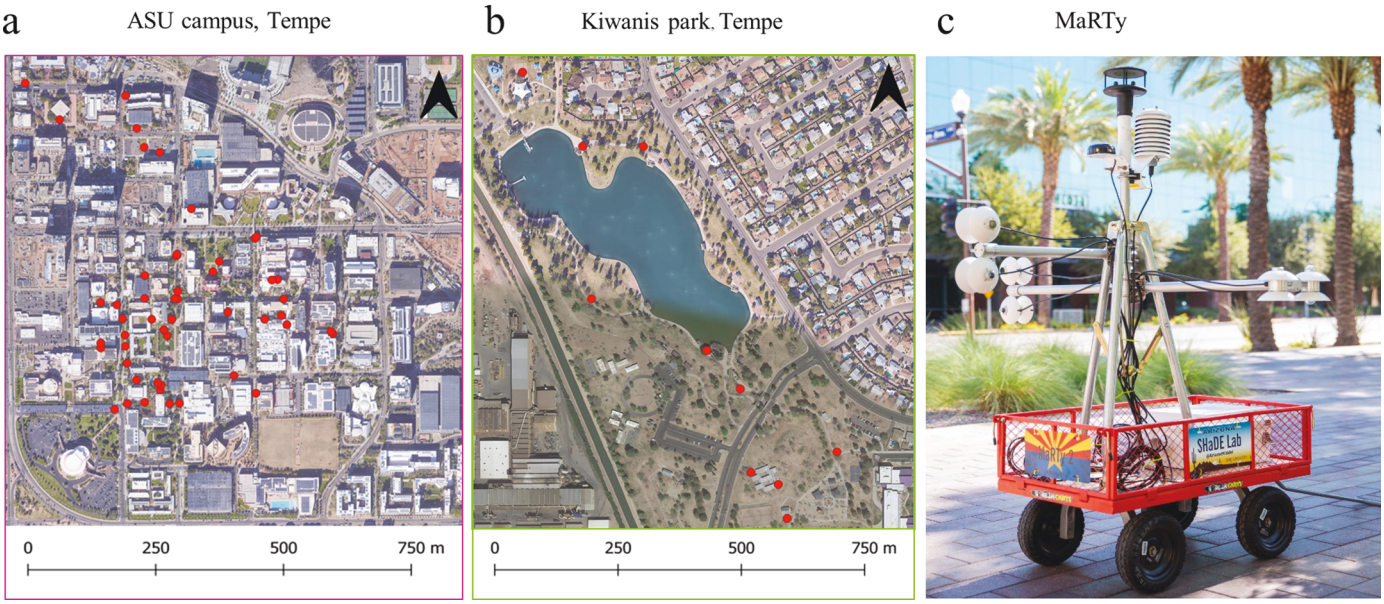

Fig. 3. a) Model validation sites on Arizona State University's Tempe campus; b) model validation sites in Kiwanis Park; c) MaRTy the biometeorological cart (Middel and Krayenhoff, 2019).

Encanto Park weather station (AZMET, 2022). The model's performance was evaluated based on exposure (sun-exposed or shaded; this classification can vary by time of day for each site) and exposure type (open, shaded by trees, shaded by building). For both analyses, we compared T_{MRT} estimates from SOLWEIG with MaRTy-observed T_{MRT} to identify linear relationships by calculating the coefficients of correlation (R) and the coefficients of determination (R^2). Furthermore, Willmott's index of agreement (d) between the modeled and the observed measurements was calculated. The index is a bounded and non-dimensional metric (Willmott, 1982). In addition, the root mean square error (RMSE), its systematic and unsystematic components, the mean absolute error (MAE), and the mean bias error (MBE) were calculated and compared with thermal stress standards set by the International Organization for Standards (ISO 7726, 1998). After the validation, hourly (07:00 h to 20:00 h) T_{MRT} maps over the Phoenix-Tempe metropolitan area were generated for June 27, 2012, a typical clear, dry, calm summer day.

3.3. Sidewalk shade analysis

The shadow function in SOLWEIG was used to generate hourly shade distribution maps for the Cities of Phoenix and Tempe for June 21, 2019, from 07:00 h to 19:00 h. The shadow function in SOLWEIG is based on the shadow-casting algorithm for DEMs developed by Ratti et al. (1999). Lindberg and Grimmond (2011) improved the algorithm to account for the influence of vegetation. The shadow-casting algorithm involves an iterative process in which a surface model continuously shifts with a height reduction at each step based on the Sun's altitude to get a shadow volume. The surface model is subtracted from the total shadow volume, and the result is reduced to a binary map where 0 indicates the presence of shade and 1 otherwise. The total shade is a function (Eq. 3) of the transmissivity of foliated vegetation for shortwave radiation (τ, here 0.03) and shadows from buildings and tree canopy (Lindberg & Grimmond, 2011):

$$Sh_i = sh_{building} - \left(1 - sh_{canopy}\right) * (1 - \tau) \quad (3)$$

For each timestep, the total shade provided by buildings and trees was calculated. To further identify what fraction of the shade was provided by buildings and vegetation, shade maps of buildings and vegetation were generated separately.

Walkable areas were identified based on street network data to estimate shade coverage for pedestrian routes. Sidewalk locations were determined by creating buffers around arterials and local streets using street width information provided in the City of Phoenix's guidelines for street design (City of Phoenix, 2009). Sidewalk polygons were then generated by creating buffers around the sidewalk centerlines using half of their respective width as the buffer sizes. The sidewalk polygons were intersected with the hourly shade maps to determine the total shade coverage on each sidewalk and the contribution of shade from buildings and vegetation at a 1-m spatial scale. The Maricopa Association of Government's Active Transportation Plan recommends that a 20-minute pedestrian route should have a minimum acceptable shade coverage of 20% (Maricopa Association of Governments, 2020).

4. Results

4.1. Evaluation of the SOLWEIG model

The model validation reveals a strong linear relationship between the modeled and observed T_{MRT}. The R-value of 0.91 indicates a high positive correlation between the two sets, with 83% (0.83) of the variance in all MaRTy observations being explained by the model. The high index of agreement (0.95) supports this as well. Considering all observations, the RMSE and MAE were 5.59°C and 4.60°C, respectively. The MBE of 1.59°C suggests that the model overestimates T_{MRT} in general.

Under shaded and sun-exposed conditions, irrespective of the urban form or exposure type, modeled and observed values positively correlate with R values of 0.75 and 0.70, respectively (Table 1). However, the percentages of variance in the observed data explained by the model for shaded (56%) and sun-exposed (49%) locations are relatively low. At shaded and sun-exposed locations, the RMSEs are 5.12°C and 6.60°C, and the MAEs are 4.47°C and 4.93°C, respectively. The results suggest that the model performs better under shaded conditions than under sun-exposed. The MBE values from Table 1 show that under shade (MBE= 3.21°C), the model is likely to overestimate T_{MRT} and underestimate (MBE= -2.28°C) under sun-exposed conditions.

The evaluation of the model for different urban forms and exposure types reveals that the model's performance under trees is the worst among the three categories considered. Under trees, the model shows a positive correlation with the observed data (R = 0.75) and an RMSE of 5.44°C, the percentage of variance explained (R^2 = 0.56) is moderate. The model tends to overestimate T_{MRT} under trees, as the MBE of 4.16°C indicates (Table 1). Under trees, most of the errors lie in the range of -4°C to 11°C with half of the errors in the range of 2°C to 7°C (Fig. 4). Outliers were as high as -10°C for trees (Fig. 4). At open sites, estimates show a much stronger positive correlation with the observations (R = 0.92, 85% of the variance explained), but the RMSE (6.23°C) is higher than for shaded locations. The model slightly underestimates at these sites, as the MBE of -1.78°C indicates. The error range (-15°C to 10°C) for open sites is the largest, with half of the sites yielding an error of -5°C to 3°C (Fig. 4). The model performs best for building canyons with an RMSE of 4.38°C. The linear relationship between the estimated and observed values is the highest, with 88% of the variance explained and a correlation coefficient of 0.94. For building canyons, the model underestimates T_{MRT} with an MBE of -0.24°C. The errors in building canyons are in the range of -9°C to 10°C with half of the errors ranging from -3°C to 2°C (Fig. 4).

4.2. Hourly mean radiant temperature and shade maps

T_{MRT} peaked at 83°C for sun-exposed locations (Fig. 5**a**). In the shade, T_{MRT} was as low as 41°C during the hottest time of the day, i.e., close to air temperature. T_{MRT} was generally lower in downtown Phoenix and Tempe, especially in the morning and afternoon, due to mid- and high-rise buildings. After sunset, T_{MRT} was close to air temperature across the study area.

Fig. 5**b** shows an example of an hourly shade distribution map (16:00 h, combining shade from trees and buildings) used to calculate shade coverage on sidewalks. Similar to T_{MRT}, shade coverage is higher in downtown areas. Shade coverage is maximized after sunrise and before sunset due to the low Sun elevation angle. Note that the dark patches of shade in the southwest and north area result from no data coverage.

Table 1
Summary of the model's overall performance under evaluated conditions: Overall, under shade, at sun-exposed locations, under trees, open sites, and building canyons.

Metric	Overall n=763	Shade n=538	Sun-exposed n=225	Trees n=407	Open sites n=257	Building canyons n=99
R	0.91	0.75	0.70	0.75	0.92	0.94
R^2	0.83	0.56	0.49	0.56	0.85	0.88
d	0.95	0.90	0.97	0.86	0.97	0.97
RMSE (°C)	5.59	5.12	6.60	5.44	6.23	4.38
RMSEs (°C)	2.86	3.30	2.72	4.30	1.84	1.71
RMSEu (°C)	4.81	3.91	6.01	3.33	5.95	4.03
MAE (°C)	4.60	4.47	4.93	4.90	4.61	3.45
MBE (°C)	1.59	3.21	-2.28	4.16	-1.78	-0.24

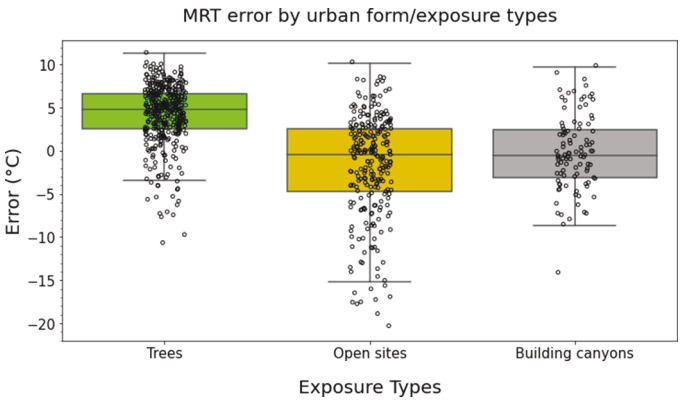

Fig. 4. Distribution of modeling errors for different exposure types.

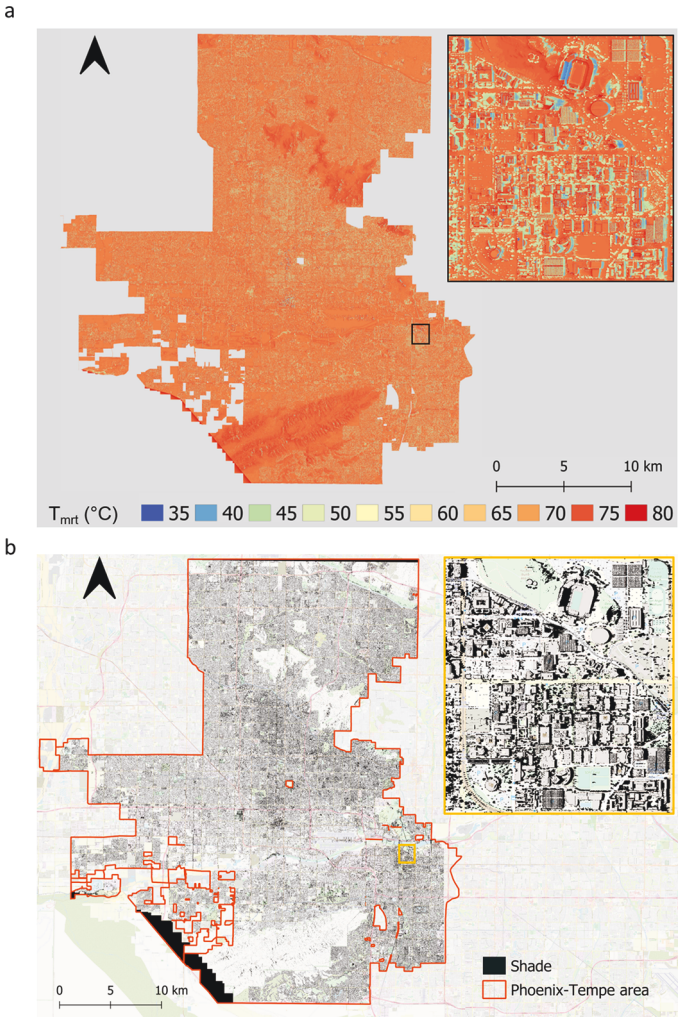

Fig. 5. a) Mean radiant temperature map of the Phoenix-Tempe area estimated for June 27, 2012, at 16:00 h; *b) Shade distribution map of Phoenix-Tempe area at 16:00 h local time on July 21, 2019, base map source: Open Street Maps.*

4.3. Assessment of sidewalk shade coverage

Fig. 6 shows the total shade coverage for selected sidewalks in Tempe Downtown for key times of the day: 07:00 h and 18:00 h (people commute to and from work or school), 16:00 h (maximum air temperature), and 12:00 h (Sun reaches the highest altitude). In the morning (Fig. 6**a**), sidewalks along the North-South direction are more shaded than sidewalks with other orientations. During mid-day, shade coverage is low for all sidewalks, with most coverage at less than 20%. Sidewalks that meet the required coverage when the Sun is at its highest altitude are mostly shaded by trees with large crowns. At the hottest time of the day, the shade coverage of all sidewalks increases because of low Sun elevation and long shadows from buildings and vegetation. In the evening, the shade coverage increases significantly for most sidewalks, even at locations with little vegetation. This shade mostly comes from buildings.

Only 8% of all sidewalks in the study area meet the 20% shade goal all day. Most sidewalks reach the 20% shade coverage target just before sunset at 19:00 h (Fig. 7). Between 08:00 h and 17:00 h, less than half of the sidewalks meet the minimum requirement. 13:00 h is when the lowest number of sidewalk corridors meet the 20 % goal.

To facilitate a neighborhood-level shade availability analysis, we calculated the total sidewalk shade coverage and shade contributions from trees versus buildings per census tract for the times of interest detailed above (Fig. 7). Census tracts with good shade coverage are mainly in the central parts of Phoenix and Tempe. Only two tracts (< 1%) have over 20% total shade coverage at all hours of the day, but all tracts meet the minimum shade goal for at least one hour. The number of tracts with a median total shade coverage of 20% or above is 84, representing 23% of the tracts. Shade coverage peaks at 19:00 h for most tracts, with a minimum at either 12:00 h or 13:00 h. Shade from vegetation accounts for the more significant part of the total shade in tracts (Fig. 8). During the day, tree shade accounts for more than 50% of the total shade in most tracts, especially at noon. The share of building shade across the study area is more significant in the mornings and evenings when the Sun elevation angle is low.

5. Discussion

5.1. SOLWEIG model validation

T_{MRT} estimates should be within ± 5 °C of observations according to the International Organization for Standardization ISO7726 standard (ISO, 1988). Following this standard, our model results can be considered adequate with an overall RMSE of 5.59°C and MAE of 4.60°C. Although the RMSE is above the standard by 0.59°C, we consider the model estimates reasonable as the effect of outliers could have influenced this value. Previous studies obtained similar results, e.g., Gál and Kántor (2020), *RMSE= 5.02°C,* and Lindberg et al. (2008), *RMSE = 4.80°C*. In addition, the high index of agreement shows that the predictions fit the observed values well (Table 1). Systematic errors (all < 5 °C) were less than unsystematic errors except for trees, which shows that the model is biased.

The model tends to overestimate T_{MRT} for shaded locations. This shortcoming is also reported by Szucs et al. (2014) and Gál and Kántor (2020). The use of domain-wide surface temperature in determining the longwave radiation and the theoretical approach with which the model estimates the fluxes from sun-exposed and shaded walls were noted as reasons for overestimations in the shade (Gál and Kántor, 2020). An imbalance in the dataset (greater number of shade/tree observations) causes our model to overestimate in general. Further analysis would be required to validate this hypothesis with a balanced observational dataset.

For sun-exposed locations, our validation shows that SOLWEIG underestimates T_{MRT} with an RMSE of 1.6 °C above the ISO standard. Underestimated downwelling radiation is the main reason for the model bias in T_{MRT} (for a detailed breakdown of up and downwelling fluxes, see supp. Fig. 1a-e). Gál and Kántor (2020) noted that lateral shortwave and longwave estimates are underestimated for sun-exposed sites.

Shade mismatch under trees, due to canopy shape errors, is a challenge in estimating T_{MRT} under trees, as the model relies on the shade distribution to estimate radiative fluxes. Shade mismatch accounts for most large errors and can be as high as 10 °C at high solar altitudes.

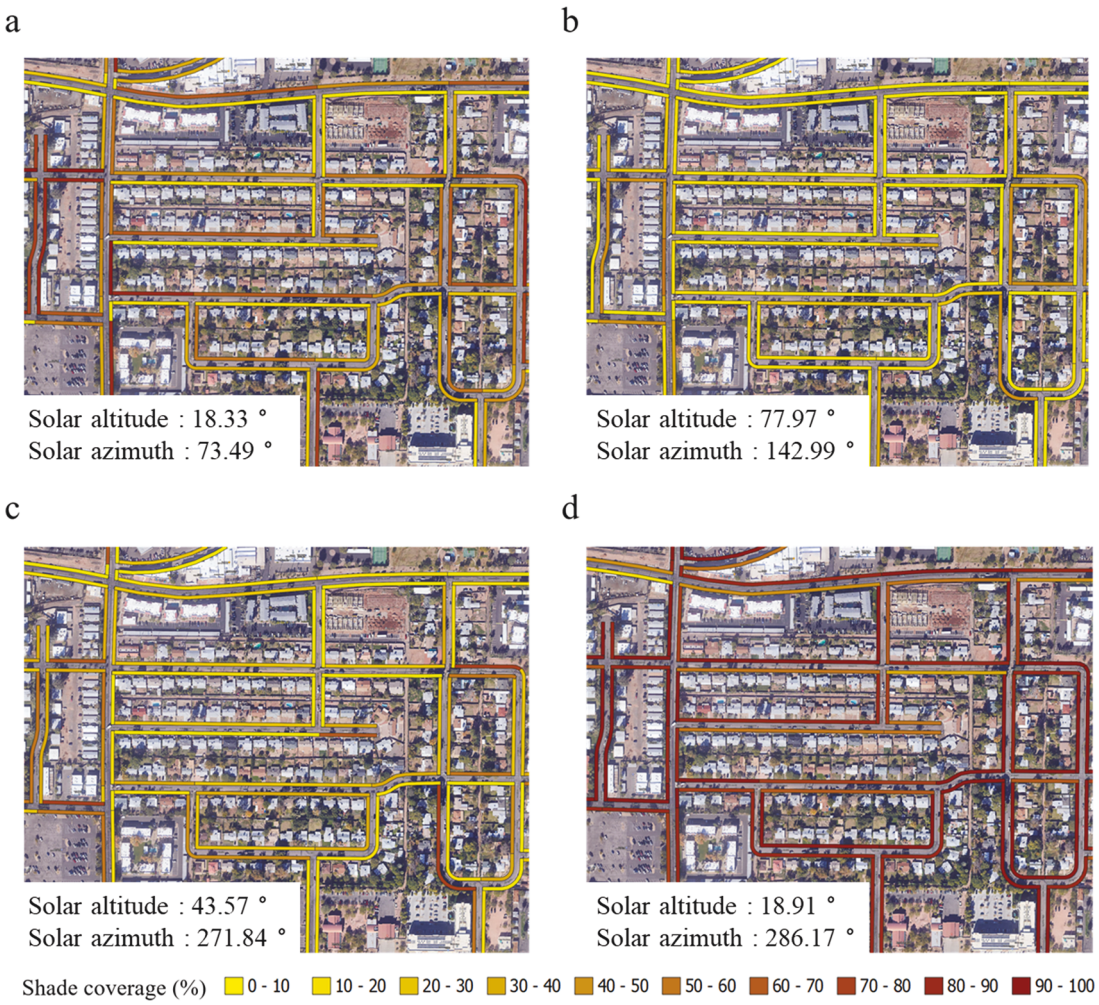

Fig. 6. Total shade coverage for selected sidewalk polygons in Tempe on June 21, 2019, a) coverage at 07:00 h; b)12:00 h; c) 16:00 h; d) 18:00 h; Sidewalk widths are enlarged in the figure for clarity.

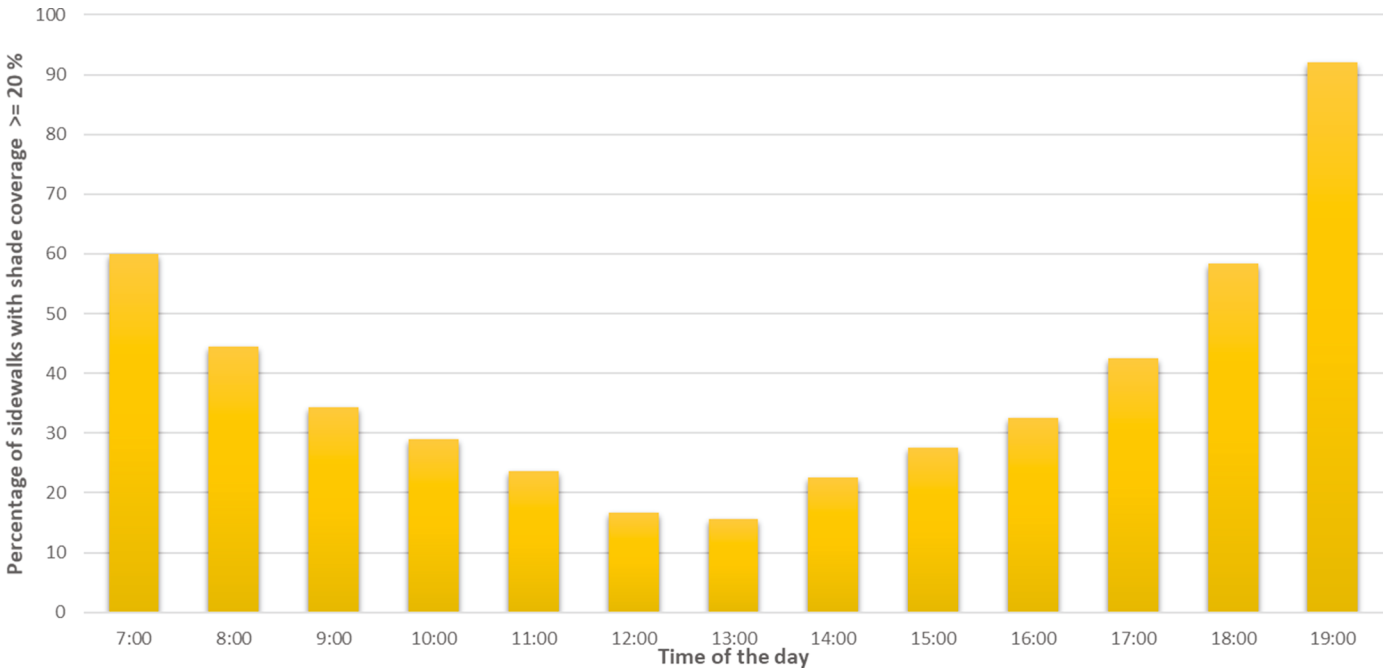

Fig. 7. The percentage of sidewalks meeting the minimum shade requirement of 20% at different times of the day.

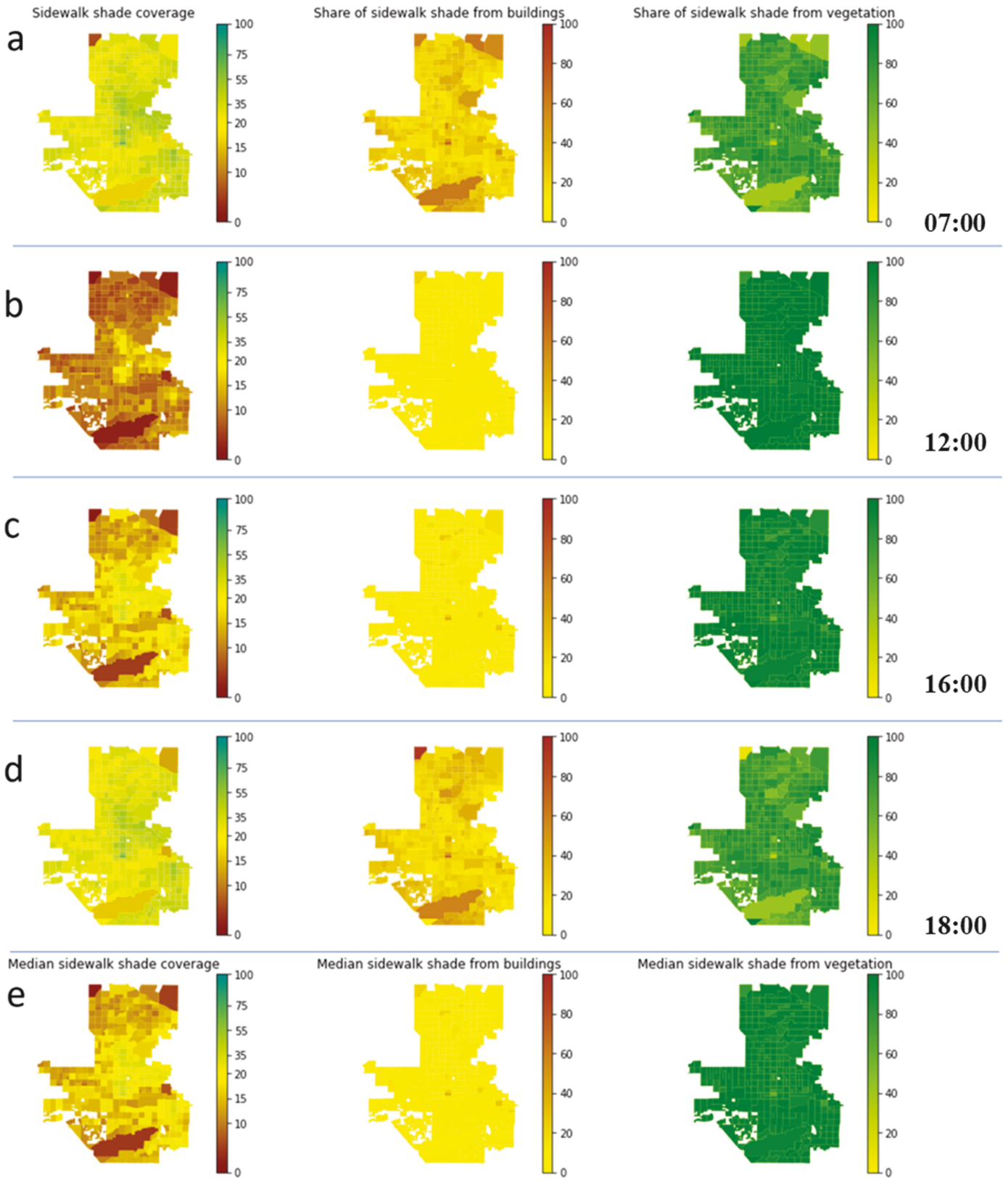

Fig. 8. Total sidewalk shade and shares contributed from buildings and vegetation per census tract in the Phoenix-Tempe area on June 21, 2019, a) coverage at 07:00 h; b)12:00 h; c) 16:00 h; d) 18:00 h; e) Median coverage per tract for the entire day. Note that the outlier census tracts (top left and right, elongated tract to the south) are mountain preserves with few residential areas.

Generating an accurate tree geometry in the CDSM is challenging as it depends on the density of the point cloud. The correct shape of tree crowns is not always obtained, which results in an inaccurate depiction of shadows. We recommend the usage of LiDAR data with high point density, especially in cities with lots of trees, to ensure the geometries of the tree crowns are adequately represented in the CDSM.

In this research, observations were made under different tree species with varying characteristics (leaf area density, canopy size, height, etc.). Azcarate et al. (2021) also indicate that transmissivity varies with the foliation density of trees. While several transmissivity values were explored to minimize RMSE, a single transmissivity value is not valid for all trees. Therefore, the T_{MRT} estimates do not match observations well under some trees.

The model performs well for building canyons, given the limited information on wall properties and the assumption of a uniform albedo for all sites. The building canyon RMSE is well in range according to the ISO standards, giving the model more credence. Again, shortwave radiation is underestimated, which was also reported by Lau et al. (2016).

In this research, additional information on the land cover was not included in the modeling processes. Previous studies found that ground surface characteristics have less influence on T_{MRT} than shading but are still relevant (Lindberg et al., 2016; Middel & Krayenhoff, 2019). Therefore, including ground surface characteristics will reduce errors in the upwelling longwave radiation and reflected shortwave radiation.

5.2. Assessment of sidewalk shade coverage

The share of sidewalks that attain the required shade coverage throughout the day indicates that most parts of the Phoenix-Tempe area are not walkable in the summer. Tracts in Phoenix and Tempe downtown have good shade coverage due to a mix of trees and tall buildings that improves shade distribution in cities (Sabrin et al., 2021). Jamei and Rajagopalan (2017) suggest that tall buildings could provide more shade and reduce T_{MRT} in downtown areas compared to trees. Outside the downtown areas, sidewalk shade coverage is poor. The share of tree shade is far greater than that of buildings because residential areas in the Phoenix area have low-rise buildings, wide roads, and high sky view factors (LCZ 6). Thermal comfort could be significantly improved in these tracts by street tree planting (Aminipouri et al., 2019; Sabrin et al., 2021; Tan et al., 2016). Studies have shown that increasing the number of street trees could reduce T_{MRT} by as much as 7 °C and reduce PET significantly (Aminipouri et al., 2019; Gál & Kántor, 2020; Lachapelle et al., 2023; Sabrin et al., 2021). A study conducted in a residential neighborhood in Freiburg found trees reduce T_{MRT} by 6.6 °C, which translates into a 3.0 °C reduction in PET (Lee et al., 2016). A similar effect can be achieved in residential areas; however, the trees would have to be mature (Sabrin et al., 2021) and may be water-use intensive, which is a trade-off in hot, dry environments (Middel et al., 2021). With advancements in computational tools, scenarios involving these tree species and other conditions could be simulated beforehand to optimize tree-planting campaigns to improve pedestrian thermal comfort (Azcarate et al., 2021; Tan et al., 2016; Wallenberg et al., 2022). Metrics such as the Shade Index used by Aleksandrowicz et al. (2020) could also be used in the planning and optimizing phase. Other urban shade sources have proven to provide similar T_{MRT} reductions, especially during the day (Middel et al., 2021), and could be employed as stopgaps while trees are growing. The shade assessments performed for sidewalks can be replicated for public spaces such as parks and playgrounds for children using the data to assess the thermal comfort at these places, as seen in Bäcklin et al. (2021).

A challenge that could be encountered in adopting our approach for other parts of the world would be the unavailability of ready-to-use sidewalk polygon data. This can be resolved by following the buffer analysis employed in this research, given the street width information. Alternatively, machine learning could be employed to extract sidewalk polygons from high-resolution aerial images.

6. Conclusions

Urban overheating is a significant challenge of the 21st century. Heat-related illness and death are preventable if the location of vulnerable populations and hyper-local biometeorological conditions are known to target heat mitigation interventions. This study advances human thermal exposure research by modeling the heat load on the human body at 1-m resolution for different exposure types (sun-exposed, shaded by trees, shaded by buildings) and urban forms under hot, dry conditions. T_{MRT} estimates from SOLWEIG were validated using extensive 6-directional field observations, yielding errors close to the ± 5°C acceptable criteria required for ISO7726. To assist local municipalities with Cool Corridor Planning, we calculated hourly shade coverage on sidewalks for a hot summer day in the Phoenix-Tempe area to identify neighborhoods that do not meet the minimum shade coverage recommendation of 20% as outlined in the Maricopa Association of Government's Active Transportation Plan. Our approach provides essential information on current shade coverage that was previously unavailable to local governments to make better-informed decisions on human-centric cooling strategies. Results will inform municipal plans to optimize shade presence, use, and effectiveness. Combined with socio-economic and demographic data, our shade and T_{MRT} maps will inform heat action plans to make cities in the metropolitan area and elsewhere more walkable, liveable, and heat-equitable. In the future, fine-scale T_{MRT} will also help assess pedestrian thermal sensation in transient environments when combined with individual travel data (Dzyuban et al., 2022; Lau et al., 2019; Li et al., 2023). Future works in this field should focus on the travel behavior of pedestrians and resulting heat exposure integrating fine-scale T_{MRT} data into travel simulation models.

Declaration of Competing Interest

The authors declare that they have no known conflicting financial interests or personal relationships that could have appeared to influence the work reported in this paper.

Data availability

Data will be made available on request.

Acknowledgements

This work was supported in by the Education and Youth Board of Estonia through the Dora+ mobility scholarships and the Ministry of Education and Research of Estonia (grant PRG-352) and the National Science Foundation, grant number CMMI-1942805 (CAREER: Human Thermal Exposure in Cities - Novel Sensing and Modeling to Build Heat-Resilience). Any opinions, findings, and conclusions or recommendations expressed in this material are those of the authors and do not necessarily reflect the views of the sponsoring organizations.

References

Acero, J. A., & Arrizabalaga, J. (2018). ENVI-met model in diurnal cycles for different meteorological conditions. *Theor Appl Climatol, 131*, 455–469. https://doi.org/10.1007/s00704-016-1971-y

Aleksandrowicz, O., Zur, S., Lebendiger, Y., & Lerman, Y. (2020). Shade maps for prioritizing municipal microclimatic action in hot climates: Learning from Tel Aviv-Yafo. *Sustainable Cities and Society, 53*(August 2019), Article 101931. https://doi.org/10.1016/j.scs.2019.101931

Aminipouri, M., Knudby, A. J., Krayenhoff, E. S., Zickfeld, K., & Middel, A. (2019). Modelling the impact of increased street tree cover on mean radiant temperature across Vancouver's local climate zones. *Urban Forestry and Urban Greening, 39* (January), 9–17. https://doi.org/10.1016/j.ufug.2019.01.016

Aviv, D., Gros, J., Alsaad, H., Teitelbaum, E., Voelker, C., Pantelic, J., & Meggers, F. (2022). A data-driven ray tracing simulation for mean radiant temperature and

spatial variations in the indoor radiant field with experimental validation. *Energy and Buildings, 254*, Article 111585. https://doi.org/10.1016/j.enbuild.2021.111585
Azcarate, I., Acero, J.Á., Garmendia, L., & Rojí, E. (2021). Tree layout methodology for shading pedestrian zones: Thermal comfort study in Bilbao (Northern Iberian Peninsula). *Sustainable Cities and Society, 72*, Article 102996. https://doi.org/10.1016/J.SCS.2021.102996
Bäcklin, O., Lindberg, F., Thorsson, S., Rayner, D., & Wallenberg, N. (2021). Outdoor heat stress at preschools during an extreme summer in Gothenburg, Sweden - Preschool teachers' experiences contextualized by radiation modelling. *Sustainable Cities and Society, 75*, Article 103324. https://doi.org/10.1016/J.SCS.2021.103324
AZMET. (2022). *The Arizona Meteorological Network*. https://ag.arizona.edu/azmet/.
Butt, A., Amati, M., Sun, C., & Deilami, K. (2019). Planning Shadeways in Bendigo : An Example of Digital Planning to Adapt to Extreme Heat' Planning Shadeways in Bendigo : An Example of Digital Planning to Adapt to Extreme Heat'. In G. Williams (Ed.), *TREENET Proceedings of the 20th National Street Tree Symposium 2019* (pp. 65–75).
Chen, Y.-C., Lin, T.-P., & Matzarakis, A. (2014). Comparison of mean radiant temperature from field experiment and modelling: a case study in Freiburg, Germany. *Theoretical and Applied Climatology, 118*(3), 535–551. https://doi.org/10.1007/s00704-013-1081-z
Crank, P. J., Middel, A., Wagner, M., Hoots, D., Smith, M., & Brazel, A. (2020). Validation of seasonal mean radiant temperature simulations in hot arid urban climates. *Science of the Total Environment, 749*, Article 141392. https://doi.org/10.1016/j.scitotenv.2020.141392
City of Phoenix. (2009). *Street Planning and Design Guidelines*. Phoenix.
Deilami, K., Rudner, J., Butt, A., MacLeod, T., Williams, G., Romeijn, H., & Amati, M. (2020). Allowing users to benefit from tree shading: Using a smartphone app to allow adaptive route planning during extreme heat. *Forests, 11*(9), 1–15. https://doi.org/10.3390/f11090998
Dzyuban, Y., Ching, G. N. Y., Yik, S. K., Tan, A. J., Banerjee, S., Crank, P. J., & Chow, W. T. L. (2022). Outdoor thermal comfort research in transient conditions: A narrative literature review. *Landscape and Urban Planning, 226*, Article 104496. https://doi.org/10.1016/j.landurbplan.2022.104496
Franklin, R., Inanc, M., & Xie, Z. (2006). Terrain Elevation Data Structure Operations. *Autocarto 2006*. https://cartogis.org/docs/proceedings/2006/franklin_inanc_xie.pdf.
Gál, C. V., & Kántor, N. (2020). Modeling mean radiant temperature in outdoor spaces, A comparative numerical simulation and validation study. *Urban Climate, 32* (December 2019), Article 100571. https://doi.org/10.1016/j.uclim.2019.100571
Guo, H., Aviv, D., Loyola, M., Teitelbaum, E., Houchois, N., & Meggers, F. (2020). On the understanding of the mean radiant temperature within both the indoor and outdoor environment, a critical review. *Renewable and Sustainable Energy Reviews, 117* (October 2019), Article 109207. https://doi.org/10.1016/j.rser.2019.06.014
Handy, S. L., Boarnet, M. G., Ewing, R., & Killingsworth, R. E. (2002). How the built environment affects physical activity: Views from urban planning. *American Journal of Preventive Medicine, 23*(1), 64–73. https://doi.org/10.1016/S0749-3797(02)00475-0, 2 SUPPL.
Hardy, J. D., & Stoll, A. M. (1954). Measurement of radiant heat load on man in summer and winter Alaskan climates. *Journal of Applied Physiology, 7*(2), 200–211. https://doi.org/10.1152/jappl.1954.7.2.200
Höppe, P. (1992). A new procedure to determine the mean radiant temperature outdoors. *Wetter Leben, 44*, 147–151.
International Organization for Standardization. (1998). *Ergonomics of the thermal environment: Instruments for measuring physical quantities (7726)*. Geneva: International Organization for Standardization.
Jamei, E., & Rajagopalan, P. (2017). Urban development and pedestrian thermal comfort in Melbourne. *Solar Energy, 144*, 681–698. https://doi.org/10.1016/j.solener.2017.01.023
Kong, F., Chen, J., Middel, A., Yin, H., Li, M., Sun, T., Zhang, N., Huang, J., Liu, H., Zhou, K., & Ma, J. (2022). Impact of 3-D urban landscape patterns on the outdoor thermal environment: A modelling study with SOLWEIG. *Computers, Environment and Urban Systems, 94*, Article 101773. https://doi.org/10.1016/J.COMPENVURBSYS.2022.101773
Krüger, E. L., Minella, F. O., & Matzarakis, A. (2014). Comparison of different methods of estimating the mean radiant temperature in outdoor thermal comfort studies. *International Journal of Biometeorology, 58*(8), 1727–1737. https://doi.org/10.1007/s00484-013-0777-1
Lachapelle, J. A., Scott Krayenhoff, E., Middel, A., Coseo, P., & Warland, J. (2023). Maximizing the pedestrian radiative cooling benefit per street tree. *Landscape and Urban Planning, 230*(October 2022), Article 104608. https://doi.org/10.1016/j.landurbplan.2022.104608
Lau, K. K. L., Ren, C., Ho, J., & Ng, E. (2016). Numerical modelling of mean radiant temperature in high-density sub-tropical urban environment. *Energy and Buildings, 114*, 80–86. https://doi.org/10.1016/j.enbuild.2015.06.035
Lau, K. K. L., Shi, Y., & Ng, E. Y.-Y. (2019). Dynamic response of pedestrian thermal comfort under outdoor transient conditions. *International Journal of Biometeorology, 63*(7), 979–989. https://doi.org/10.1007/s00484-019-01712-2
Lee, H., Mayer, H., & Chen, L. (2016). Contribution of trees and grasslands to the mitigation of human heat stress in a residential district of Freiburg, Southwest Germany. *Landscape and Urban Planning, 148*, 37–50. https://doi.org/10.1016/J.LANDURBPLAN.2015.12.004
Li, R., Chester, M. V., Middel, A., Vanos, J., Hernandez-Cortes, D., Buo, I., & Hondula, D. M. (2023). Effectiveness of Travel Behavior and Infrastructure Change to Mitigate Heat Exposure. *Frontiers in Sustainable Cities* [under review].
Lindberg, F., & Grimmond, C. S. B. (2011). The influence of vegetation and building morphology on shadow patterns and mean radiant temperatures in urban areas: Model development and evaluation. *Theoretical and Applied Climatology, 105*(3), 311–323. https://doi.org/10.1007/s00704-010-0382-8
Lindberg, F., Holmer, B., & Thorsson, S. (2008). SOLWEIG 1.0 - Modelling spatial variations of 3D radiant fluxes and mean radiant temperature in complex urban settings. *International Journal of Biometeorology, 52*(7), 697–713. https://doi.org/10.1007/s00484-008-0162-7
Lindberg, F., Onomura, S., & Grimmond, C. S. B. (2016). Influence of ground surface characteristics on the mean radiant temperature in urban areas. *International Journal of Biometeorology, 60*(9), 1439–1452. https://doi.org/10.1007/s00484-016-1135-x
Maricopa Association of Governments. (2020). *MAG active transportation plan*.
Middel, A., Alkhaled, S., Schneider, F. A., Hagen, B., & Coseo, P. (2021). 50 Grades of Shade. *Bulletin of the American Meteorological Society*, 1–35. https://doi.org/10.1175/bams-d-20-0193.1
Middel, A., & Krayenhoff, E. S. (2019). Micrometeorological determinants of pedestrian thermal exposure during record-breaking heat in Tempe, Arizona: Introducing the MaRTy observational platform. *Science of The Total Environment, 687*, 137–151. https://doi.org/10.1016/J.SCITOTENV.2019.06.085
Middel, A., Selover, N., Hagen, B., & Chhetri, N. (2016). Impact of shade on outdoor thermal comfort—a seasonal field study in Tempe, Arizona. *International Journal of Biometeorology, 60*(12), 1849–1861. https://doi.org/10.1007/s00484-016-1172-5
Nazarian, N., Krayenhoff, E. S., Bechtel, B., Hondula, D. M., Paolini, R., Vanos, J., Cheung, T., Chow, W. T. L., de Dear, R., Jay, O., Lee, J. K. W., Martilli, A., Middel, A., Norford, L. K., Sadeghi, M., Schiavon, S., & Santamouris, M. (2022). Integrated Assessment of Urban Overheating Impacts on Human Life. *Earth's Future, 10*(8). https://doi.org/10.1029/2022EF002682
Oke, T. R. (1981). Canyon geometry and the nocturnal urban heat island: Comparison of scale model and field observations. *Journal of Climatology, 1*(3), 237–254. https://doi.org/10.1002/joc.3370010304
Ratti, C., Di Sabatino, S., & Britter, R. (1999). Urban Texture Analysis with Image Processing Techniques Carlo. *CAADFutures, 99*.
Sabrin, S., Karimi, M., Nazari, R., Pratt, J., & Bryk, J. (2021). Effects of Different Urban-Vegetation Morphology on the Canopy-level Thermal Comfort and the Cooling Benefits of Shade Trees: Case-study in Philadelphia. *Sustainable Cities and Society, 66* (December 2020), Article 102684. https://doi.org/10.1016/j.scs.2020.102684
Seneviratne, S. I., Nicholls, N., Easterling, D., Goodess, C. M., Kanae, S., Kossin, J., Luo, Y., Marengo, J., Mc Innes, K., Rahimi, M., Reichstein, M., Sorteberg, A., Vera, C., Zhang, X., Rusticucci, M., Semenov, V., Alexander, L. V., Allen, S., Benito, G., … Zwiers, F. W. (2012). Changes in climate extremes and their impacts on the natural physical environment. *Managing the Risks of Extreme Events and Disasters to Advance Climate Change Adaptation: Special Report of the Intergovernmental Panel on Climate Change, 9781107025*, 109–230. https://doi.org/10.1017/CBO9781139177245.006
Speak, A., Montagnani, L., Wellstein, C., & Zerbe, S. (2021). Forehead temperatures as an indicator of outdoor thermal comfort and the influence of tree shade. *Urban Climate, 39*(March), Article 100965. https://doi.org/10.1016/j.uclim.2021.100965
Szucs, Á., Gál, T., & Andrade, H. (2014). Comparison of measured and simulated mean radiant temperature. Case study in Lisbon (Portugal). *Finisterra, 49*(98), 95–111. https://doi.org/10.18055/Finis6469
Tabatabaie, S., Litt, J. S., & Carrico, A. (2019). A study of perceived nature, shade and trees and self-reported physical activity in Denver. *International Journal of Environmental Research and Public Health, 16*(19). https://doi.org/10.3390/ijerph16193604
Tan, Z., Lau, K. K. L., & Ng, E. (2016). Urban tree design approaches for mitigating daytime urban heat island effects in a high-density urban environment. *Energy and Buildings, 114*, 265–274. https://doi.org/10.1016/J.ENBUILD.2015.06.031
Vanos, J. K., Rykaczewski, K., Middel, A., Vecellio, D. J., Brown, R. D., & Gillespie, T. J. (2021). Improved methods for estimating mean radiant temperature in hot and sunny outdoor settings. *International Journal of Biometeorology, 65*(6), 967–983. https://doi.org/10.1007/s00484-021-02131-y
VDI. (1998). *Methods for the Human-Biometeorological Assessment of Climate and Air Hygiene for Urban and Regional Planning. Part 1: Climate. DI 3787, Part 2*.
Wallenberg, N., Lindberg, F., & Rayner, D. (2022). Locating trees to mitigate outdoor radiant load of humans in urban areas using a metaheuristic hill-climbing algorithm - introducing TreePlanter v1.0. *Geoscientific Model Development, 15*(3), 1107–1128. https://doi.org/10.5194/gmd-15-1107-2022
Wang, C., Middel, A., Myint, S. W., Kaplan, S., Brazel, A. J., & Lukaszyk, J. (2018). Assessing local climate zones in arid cities: The case of Phoenix, Arizona and Las Vegas, Nevada. *ISPRS Journal of Photogrammetry and Remote Sensing, 141*, 59–71. https://doi.org/10.1016/j.isprsjprs.2018.04.009
Willmott, C. J. (1982). Some comments on the evaluation of model performance. *Bulletin of the American Meteorological Society, 63*(11), 1309–1313. https://doi.org/10.1175/1520-0477(1982)063<1309:SCOTEO>2.0.CO;2